Liquid Metal Gallium in Metal inserts for Solar Thermal Energy Storage: A Novel Heat Transfer Enhancement Technique

Srikanth Salyan[a], Praveen B[a], Harjit Singh[b], S. Suresh[a]*, A Sarath Reddy[a]

[a]Department of Mechanical Engineering, National Institute of Technology, Tiruchirappalli – 620015, Tamil Nadu. India.

[b]Brunel University London, Kingston Lane Uxbridge, Uxbridge UB8 3PH, UK

Mail: srikanthsalyan@gmail.com, praveennitt15@gmail.com, harjit.singh@brunel.ac.uk, ssuresh@nitt.edu, sarathreddy11@outlook.com

*- Corresponding Author

Abstract

This paper investigates the heat transfer characteristics of a prototype latent heat energy storage (LHES) system with novel metal insert design configuration. The novel thermal energy storage (TES)system consist ofa vertical cylindrical shell, a helical coil and metalinserts (MI) withliquid metal gallium(Ga), designed for LHES capacity of ~13MJ. 25 kg of D-Mannitol(DM) is investigated as a phase change material (PCM) forenergy storage and property tests were conducted on DM. PCM was cycled 1000 times and checked for suitability for long term energy storage applications. Results confirmed that the addition of MI with Ga enhanced the thermal performance of the TES system. Moreover, the vertical orientation of the shell as well as the metal inserts supported natural convection during charging cycles and acted as a nucleation sites during discharging cycles, thereby assuring rapid charging and discharging of the TES system. High thermal conductivity, low specific heat of Ga and its liquid phase atroom temperatures helped Ga act as thermal energy carriers in TES unit. Maximum power output of 0.64 kW was obtained during solidification cycle and efficiency range of 87-89% for MI configuration. The presented novel LHES design can be used with a wide range of PCM and over a different temperature range of applications, mainly for water heating, high temperature industrial waste heat recovery and solar thermal applications.

Keyword

Latent heat storage system, Liquid Metal Gallium, Metal Inserts, Energy Efficiency.

Abbreviation

CDH	Central Drug House
DM	D-Mannitol
DSC	Differential scanning calorimetry
EG	Expanded graphite
FT-IR	Fourier Transform Infra-red
Ga	Gallium
HTF	Heat transfer fluid
LFA	Laser flash apparatus
LM	Liquid Metal

Greek Symbol

β	Beta Polymeric Phase of D-Mannitol
η	Efficiency

Nomenclature

T	Temperature(°C)
k	Thermal conductivity(W/m·K)
m	Mass (kg)
u	Independent variable
Q	Energy (J)
N	Performing parameter
P	Mean Power

Subscript

s	Solid
m	Melting point

l Liquid

1. Introduction:

Energy consumption in the world has increased gradually and significantly due to the ever-expanding demand for human activity. In this light, to decrease the gap between energy demand and supply, and to enhance the energy efficiency of current system, thermal energy storage (TES) is a promising candidate [1-3]. Latent heat energy storage is a significant part of TES due to its ability to store large amounts of energy at a constant temperature. Phase change material (PCM) undergo solid-liquid, solid-solid or solid-gas transformations which store huge amounts of energy during phase change at nearly isothermal temperatures [4-5]. Solid-liquid PCMs are widely used in practical application due to their availability over awide temperature range, high latent heat capacity and cheap costs. One of the drawbacks include volumetric expansion during phase change. Moreover, the lower thermal response of the PCM due to lower thermal conductivity values is a bigger challenge to researchers. Many efforts have been done to study the mechanism of heat transfer during solid-liquid phase changes [6]. It is therefore important to improve energy storage/retrieval, which in turn enhances the efficiency of the system. LHES can be broadly classified into low, medium and high temperature storage systems [7]. For low temperatures in the range of 20-90 ^{O}C, paraffin are the most desired PCM [8]. However, the low thermal conductivity (< 0.4 W/m·K) is the drawback which limits its usage [9]. One of the methods to enhance the thermal conductivity of the PCM is by adding high thermal conductivity materials to the PCM. The additives vary from micron to nano sizes and are commonly used in the form of metal oxides, carbon based and pure metal particles [10-14]. However, the addition of these additives leads to a decrease in the latent heat capacity of the PCM. Sari et al. [15] investigated the effect of paraffin with expanded graphite (EG) as a phase change composite and found that the composite showed very good thermophysical properties with stable chemical properties, enhanced thermal conductivity and satisfactory latent heat storage system. Ranjbaret al. [16] studied the heat transfer behaviour in a 3D cavity setup with the addition of nanoparticles. The results showed a substantial increase in heat transfer after the addition of the particles. Hosseinizadeh et al. [17] investigated the melting of nano-enhanced phase change materials inside a spherical container. The PCM used was paraffin laden with copper particles as thermal conductivity enhancer. Results showed that with increase in thermal conductivity of the NEPCM and

decreased latent heat, the melting rate of the NEPCM was very high as compared to the case where pure PCM was used. Rabienataj et al. [18] studied the impact of heat transfer tube eccentricity on the performance of the LHES. Melting behaviour of PCM was investigated using a numerical model with shell and tube configuration. Results were compared with concentric and eccentric type heat transfer tubes. The heat exchanger with eccentric configuration wherein the tube was shifted below the axis, showed greater melting performance due enhanced natural convection. Ismail et al. [19] studied the enhancement of heat transfer during solidification using axial fins. They studied the effect of different fin height and fin thickness on the performance of TES. Hosseini et al. [20] conducted a comparison of experimental and numerical investigation of TES and studied the effect of change of inlet temperature on the theoretical efficiency of the heat exchanger. From the results it was seen that by increasing the inlet temperature from 70 °C to 75 °C, the efficiency of the system improved from 81.1% to 88.4% respectively. Vyshak et al. [21] analysed with numerical model the effect of different shape configuration of LHES with the same volume of PCM and the same surface area of Heat transfer. The authors presented the variation in melting time of the PCM in rectangular, cylindrical, shell and tube configurations. From the results obtained they concluded that the cylindrical configuration performed the best as compared to the other two types and the effect of shape was more relevant when the mass of PCM was increased. Adine et al. [22] investigated the use of multiple PCM with different melting points in a heat exchanger. They compared the performance of the latent heat storage unit with single PCM system and two PCM systems. Results showed that the multiple PCM systems works more efficiently when the mass flow rate is in the lower range. Gerard et al. [23] evaluated the concept of multiple phase change materials configuration using PCM with phase transition temperature in the range of 150 – 200 °C. D-Mannitol and hydroquinone is used as PCM with medium range of phase change temperatures. Tests were conducted with single PCM as well as with multiple PCM in a pilot plant scale setup and results showed that the multiple PCMs configuration enhanced the effectiveness by19.6% as compared to the single PCM configuration. Moreover, there was better uniformity between the HTF temperature difference between inlet and outlet. Rahimi et al. [24] conducted the thermal enhancement study of TES by using fin configuration. Experiments were conducted at various operating conditions and investigation showed that regardless of flow regime, the inclusion of fin enhanced the heat transfer and change in fin pitch did not affect the performance of the TES majorly. Esapour et al. [25] numerically investigated multi tube latent heat storage systems for different geometrical and operational parameters. From the

results, it was concluded that as the number of tubes increased inside the shell, the performance of the TES also increased. The design where the tubes occupy the upper part of TES takes the maximum time for melting while with the same inner tube numbers, in the lower part of the TES, melted faster. Zakir et al. [26-27] experimentally investigated the charging/discharging cycle of PCM with a novel design, longitudinal fin tube with paraffin as thermal energy storage material. Results showed that vertical arrangement of longitudinal fins supported the natural convection in PCM which enhanced the charging of TES effectively. The mean power increased by an amount of 50% and 69% as the temperature during charging is changed to 67 °C from 52 °C. Similarly, the power enhanced by 39.05% during solidification as inlet temperature was changed to 5 °C from 15 °C. Ahmad et al. [28] studied the suitability of using D-Mannitol as a PCM for medium temperature TES systems. While characterisation using DSC showed DM to have a high enthalpy of phase change of 297 kJ/kg with sufficient amount of subcooling. On the contrary, experimental results in large scale TES showed that the PCM solidified above 150 °C which suggests possibility of usage as PCM with very high latent heat capabilities.

From the literature survey, it is reviewed that most of the research work was concentrated more on enhancing the thermal performance of TES mostly by two methods (1) By adding high thermal conductivity additives to PCM (2) By incorporating fins to increase the heat transfer area between the HTF and PCM. However, in the former case, it is seen that the enthalpy of PCM is comprised by addition of particles while the later increases the weight of the TES and complexity of assembly and maintenance of the heat exchanger.

In this work, the aim is to conduct a series of experiments with DM, to draw an effective conclusion about the performance and applicability of DM as PCM. Thermo physical property study is done using various characterization techniques and the effect of thermal cycling on DM is discussed in this paper. Moreover, a novel TES design is proposed wherein gallium in metal inserts is assembled inside the TES and the effects on performance of TES is tested. Thermal behaviour in macro scale TES system is studied and the feasibility of using the novel design TES with any PCM available, for any temperature range of operation is investigated for real world conditions.

2. Methods

2.1 Material Purchased

D-Mannitol (99% Pure) was supplied by SC limited, India. Gallium, 99.97 % pure, was supplied by CDH Limited, India. All samples were reagent analytical grade and no further processing was done before use. The pictorial view of materials used in this project is shown in Fig. 1.

(a) **(b)**

Fig. 1. (a) D-Mannitol (b) Gallium

2.2 CharacterizationTechniques

The SEM technique (Make: Vega 3 Tescan) was used to study the morphology of the samples. Polymorphic structure of the DM was studied using XRD diffraction technique and comparison of the results with JCPDS. The XRD was performed using Rigaku Ultima IV XRD Model. The sample went through repeated cycling tests up to 1000 thermal cycles using a flat plate heater and autotransformer setup. 250 grams were taken as a sample size for cycling in stainless steel crucible with the lid covered by aluminium foil to prevent oxidation of PCM at high temperature liquid phases. Tests were conducted after thermal cycles to determine the change in nature and property of the PCM and suitability of usage in PCM application. Phase change properties were studied in a differential scanning calorimeter (Make: NETZSCH) at a 10 °C/min scanning rate. Nitrogen gas, with 25 ml/min flow rate was used to avoid oxidation of samples. Aluminium cell (Sealed-piercing) with 2mg PCM weight was used as sample holder. The sample weight measurement accuracy of the device is 0.01mg. Fresh samples and thermal cycled sampled were tested for their phase change characteristics. Prior to sample testing, the calibration of the DSC instrument was done by using zinc and indium standards. The phase change properties were measured during the second run and average latent heat values from three consecutive readings are presented.

Thermo gravimetric analysis (TGA-Perkin Elmer)was used to investigate the decomposition temperature above the melting point of the samples. Samples were tested up to550 °C until complete evaporation of the samples. In this approach, we measured the weight loss of DM with increase in its temperature. The thermal conductivity of the solid was measured at 25° C (RT) using LFA technique. For solid samples, pellet of 25mm size was developed using a pelletiser and all the samples was coated with graphite spray for better absorptivity during testing of the sample. To study the chemical stability of cycled PCM, Fourier Transform Infrared spectroscopy tests were conducted using Perkin Elmer Spectrometer. Tests were conducted in the wave number range of 4000 to 500 cm^{-1}.

2.3Experimental Setup- TES Prototype

In order to study the charging and discharging performance of the TES unit, a shell and helical tube system was designed and assembled. Fig. 2 (a-b) illustrates the schematic diagram and pictorial view of the experimental setup, which essentially consists of the heat transfer fluid control system, the TES section and the data acquisition system. The TES consists of a long vertical cylindrical shell made out of borosilicate glass. The shell is made from glass to enable the visualisation of melting and solidification of the PCM during experimentation. The dimensions of the glass shell are1050mm in length and 160 mm in diameter and can hold a maximum amount of 28 kg of DM. However, we have only tested with25 kg of DM for our experimentation. The helical HTF tube is embedded in the PCM storage shell and is made of copper having a pitch of 7cm and helix of 6 degrees. The tube has an internal diameter of 5mm and a thickness of 1.5 mm. The metal inserts are also made of copper with an internal diameter of 8mm and external diameter of 10mm with length of 1200mm. 150 ml of Ga is added to each tube during experimentation. A total of four such separate tubes are used for the study. Fig. 2c shows the schematic diagram of the novel TES system. The heat transfer fluid control system consists of two fluid loops i.e. the charging and the discharging loop. In the charging loop, heat is transferred from hot HTF to PCM, while in the discharging loop, the energy from PCM is transferred back to the cold HTF. The heating unit consists of an oil storage tank with a 100 litre capacity. The HTF used in this experiment is therminol -55 oil. The properties of HTF in Table. 1 are as given by the supplier's data hand book. The purpose of the heating unit is to supply large quantities of HTF at the required constant temperature to the TES during operation. During the charging process, the HTF is heated to the required temperature using a 2.5 kW, electrical resistance type heater. The input to the heater was controlled by a temperature controller via feedback from the oil

storage tank temperature. A Roto fluid twin gear pump fluid pump is used to supply the HTF through the loops. A variable speed controller is attached to the pump to control the flow velocity of the HTF. A high temperature liquid flow metre (Make: Titan) with a maximum operating temperature of 450 °C with a flow meter range of 0.1 to 10 l/min was used for measuring the flow rate of the HTF with an accuracy of 1.5%. All the thermocouples used in this experiment were connected to a data logger (KEYSIGHT). Ten thermocouples are placed in the PCM space while one each is placed at the inlet and outlet of the HTF coil to measure the inlet and outlet HTF temperature respectively. Fig. 2d shows the placement of thermocouples at various locations in the TES.

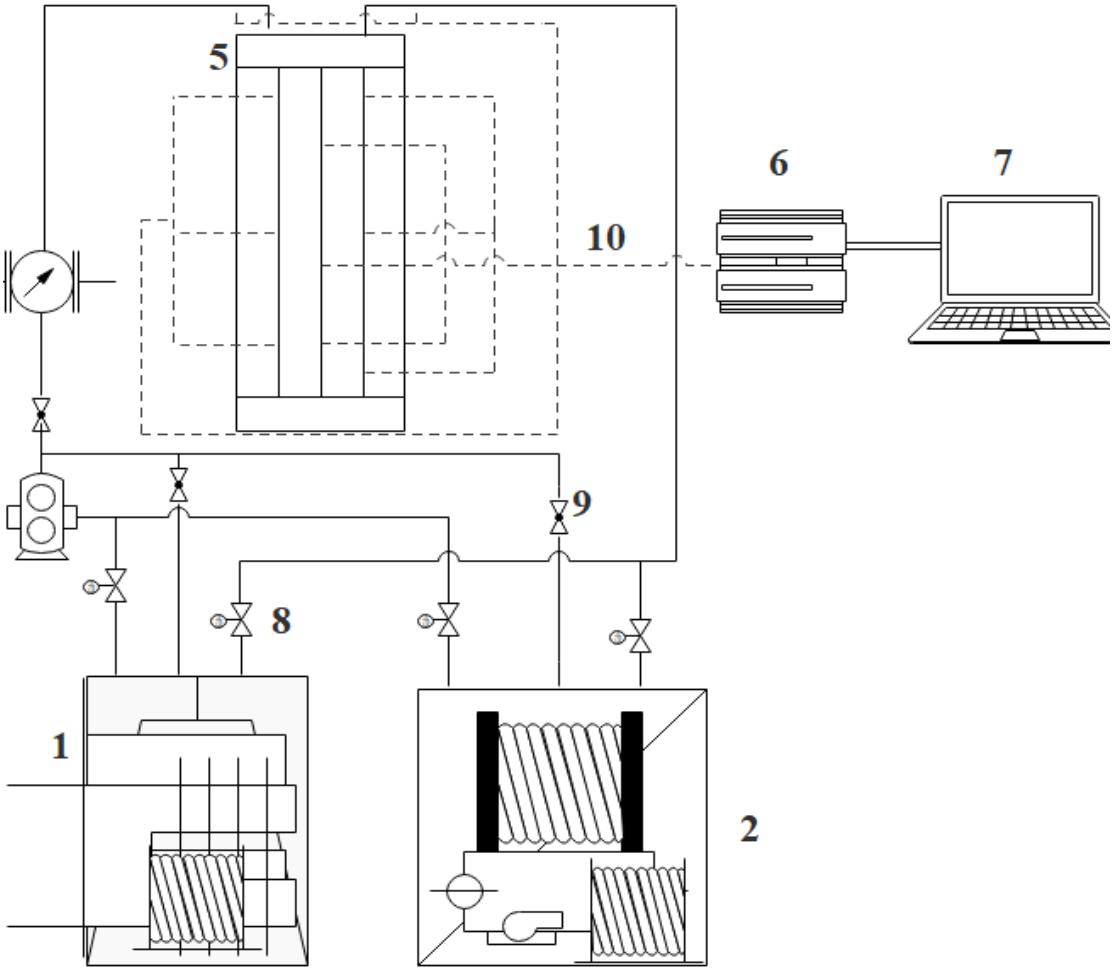

1. Chiller Unit 2. Heating Unit 3. Gear Pump

4. Flow Meter 5. TES 6. Data logger

7. Computer 8. Valve 9. Valve(Unidirectional)

10. Thermocouples

Fig. 2a. Schematic Diagram of setup

Fig. 2b. Pictorial View of Experimental Setup

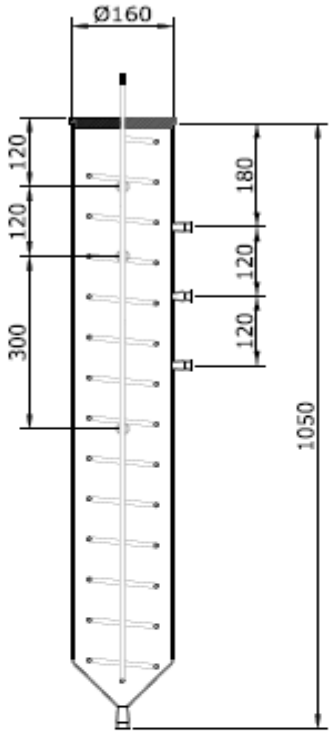

Sectional View A-A'

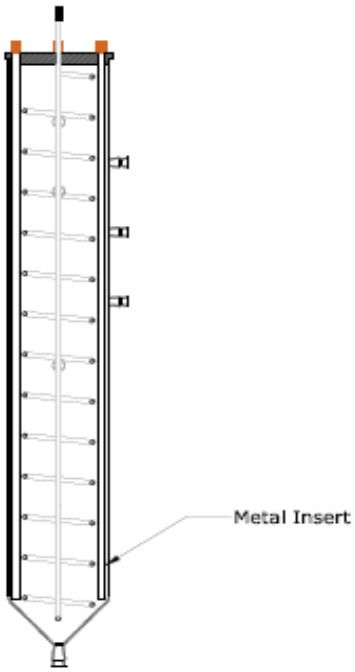

Sectional View B-B'

Top View

Without Inserts

Top View

With Inserts

Fig. 2c. Schematic Diagram showing with and without metal inserts.

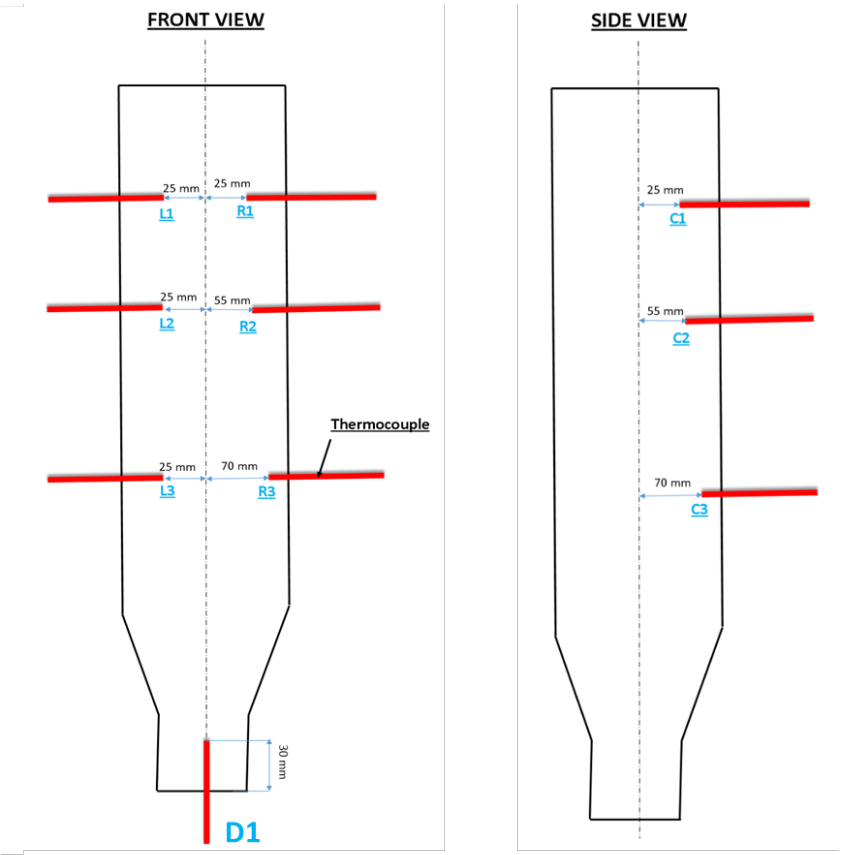

Fig. 2d. Locations of thermocouples.

Table 1. Therminol 55 - Thermo physical properties.

Specific heat (kJ/kg.K)	2.17 @ 200 °C 1.81 @ 20 °C
Density (kg/m^3)	822 @ 200 °C 890 @ 20 °C
Liquid Viscosity (cP)	0.718 @ 200 °C

2.4 Experimental Procedure:

The experimental procedure can be divided into two; the charging and the discharging process. Before the commencement of the charging process, the HTF was heated up to the desired inlet temperature of the charging process. For maintaining a uniform temperature of the HTF, the oil is circulated by the pump using a bypass line so that the HTF doesn't enter the TES prototype. The charging process commenced when the boiler temperature reached

the set temperature. The charging process was stopped once all the thermocouples show similar temperatures and the HTF temperature difference has reached a steady state. Once the TES is fully charged, the charging loop was disconnected from the TES and the valve opening the discharging loop was brought inline. The HTF was maintained at the desired discharging temperature by a chiller unit, for the discharging process. 30 °C and 20 °C were chosen as inlet temperatures of the HTF. The same procedure was used for testing the charging and discharging performance of TES with metal inserts.

2.5 Data reduction

The total energy stored by the PCM is expressed by Eq. (1).

$$Q_{theoretical} = m_{pcm} [C_{p,s} (T_m - T_f) + \Delta h_m + C_{p,l} (T_f - T_m)] \quad (1)$$

The inlet and outlet temperature of the HTF were measured with a time gap of; $\Delta t = 5s$.

Assuming negligible heat loss from the unit, the energy charging/discharging is expressed by Eq. (2).

$$Q_{charging,\ discharging} = m_{HTF}.\ C_{p.HTF} (T_{in} - T_{out}) \quad (2)$$

The total cumulative energy ($Q_{cumulative}$) calculated for the complete charging and discharging is expressed by Eq. (3).

$$Q_{cumulative} = \sum \Delta t\ .(m)_{HTF}\ .C_{p,HTF}\ .(T_{in} - T_{out}) \quad (3)$$

The mean power is evaluated by Eq. (4):

$$P_c = \frac{Q_{charging}}{t_c} \quad (4)$$

$$P_d = \frac{Q_{discharging}}{t_d}$$

The theoretical efficiency of TES is ratio of energy stored and discharged by the TES as compared to maximum possible energy stored and discharged capacity of the PCM.

$$\eta_{theoretical} = \frac{Q_{cumulative}}{Q_{theoritical}} \quad (5)$$

The total efficiency of the TES is the ratio of energy discharge to energy stored by the TES for a particular operating parameter

$$\eta_{total} = \frac{Q_{discharging}}{Q_{charging}} \quad (6)$$

2.6. Uncertainty Analysis

The thermocouple calibrator, data acquisition system, and thermocouples, have an uncertainty range of ± 0.25 °C, ± 0.20 °C, ± 0.2 °C, respectively.TGA has temperature uncertainty of ± 0.2 °C and weight sensitivity of ± 0.2 mg. DSC instrument has an accuracy of ± 0.2 °C for temperature measurements and ± 1.5 % for enthalpy measurements. Thermal diffusivity and thermal conductivity measurement has maximum uncertainties of ± 2 % and ± 5 %. The uncertainty associated with the flow meter is ± 3 %. The uncertainty of the cumulative energy stored/ discharged is calculated using the Kline- McClintock's method [29] given by the equation (7).

$$\Delta N = \sqrt{\Sigma [\frac{\partial N}{\partial u_n} . \Delta u_n]^2} \quad (7)$$

Accordingly, the maximum uncertainty estimated for energy stored and discharged is ±12.6 kJ respectively.

3. Results and Discussion

3.1 PCM Characterization

Fig. 3a shows the SEM image of DM. From the images it can be seen that DMis very irregular in shape in microstructure level. Fig 3bshowsthe XRD pattern of pristine DM. Two major peaks are seen at 23.71 and 19.08. By comparing the data obtained from JCPDS (22-1797), the β phase polymorphic state can be inferred. This is the most stable phase of DM.

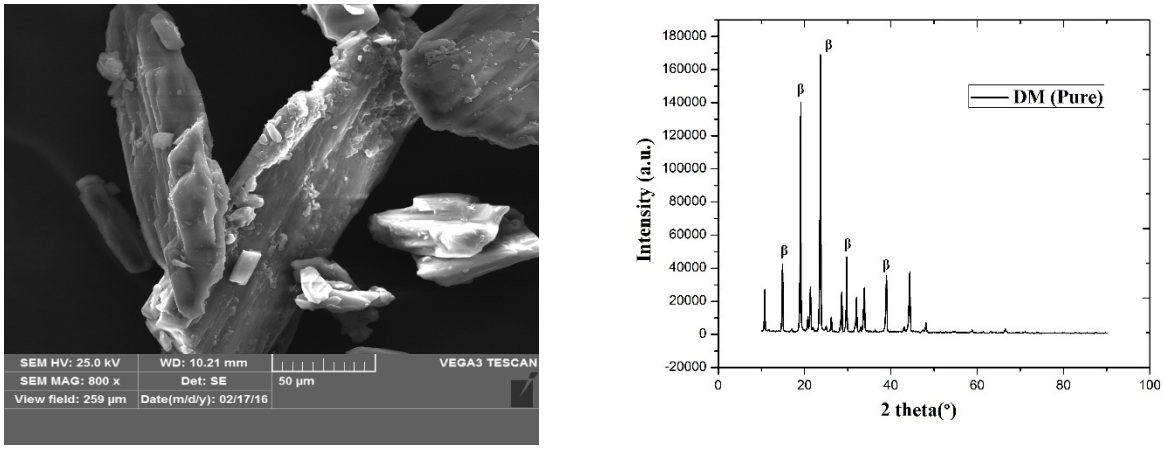

(a) **(b)**

Fig. 3. DM (a) SEM image (b) XRD spectra

Fig. 3c shows the TGA data for uncycled and 1000 thermal cycled DM. DM was stable up to 300 °C with a mass loss of less than 2%. One step mass loss happens above 310 °C which is due to the decomposition of organic compounds. This shows that there wasa wide window between the melting point and decomposition point of the sample. Hence local overheating of the sample above the melting temperature of the DM will not affect the thermal stability of the PCM in TES. After thermal cycling, the sample showed a narrowed window of decomposition temperature. The trigger for decomposition was at 240 °C with one step decomposition as seen in fresh samples. From the data, it is seen that DM is stable up to 200 °C. Laser flash technique is a widely accepted technique for the measurement of thermal conductivity and used by many researchers. [30-31]. For testing purpose, the sample were palletised to a diameter of 24.5 mm and 2mm thickness. Graphite spray was coated on the samples for accurate readings. Maximum of 3 samples were tested and average of all 5 different readings are presented. Similar procedure is followed for property measurement for thermally cycled PCM. Fig. 3d presents the thermal conductivity value after thermal cycling. Pure DM showed a value of 1.3 W/m·K. The value obtained is close to the value reportedby Palomo et al. [32]. After 350 and 1000 thermal cycles of DM, the thermal conductivity value decreased by 3.9 % and 7.6%to values of 1.25 and 1.21 W/m·K, respectively. This slight decrease in value may be neglected and attributed to the oxidation of samples after repeated thermal cycles. Fig. 3d also shows the specific heat capacity of DM before and after thermal cycles. The value was found to be 1.52 kJ/kg. K for pure DM and the value decreased by 20.39 % to 1.21 kJ/kg.K after 1000 thermal cycles.

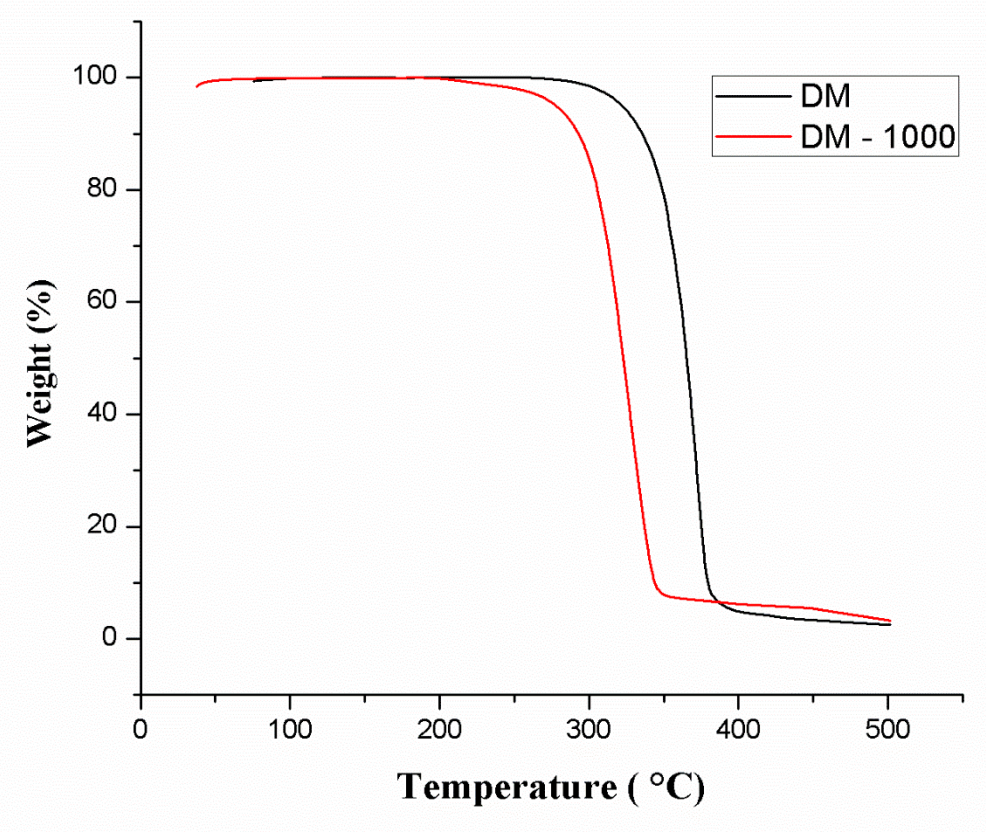

Fig. 3c. TGA of DM.

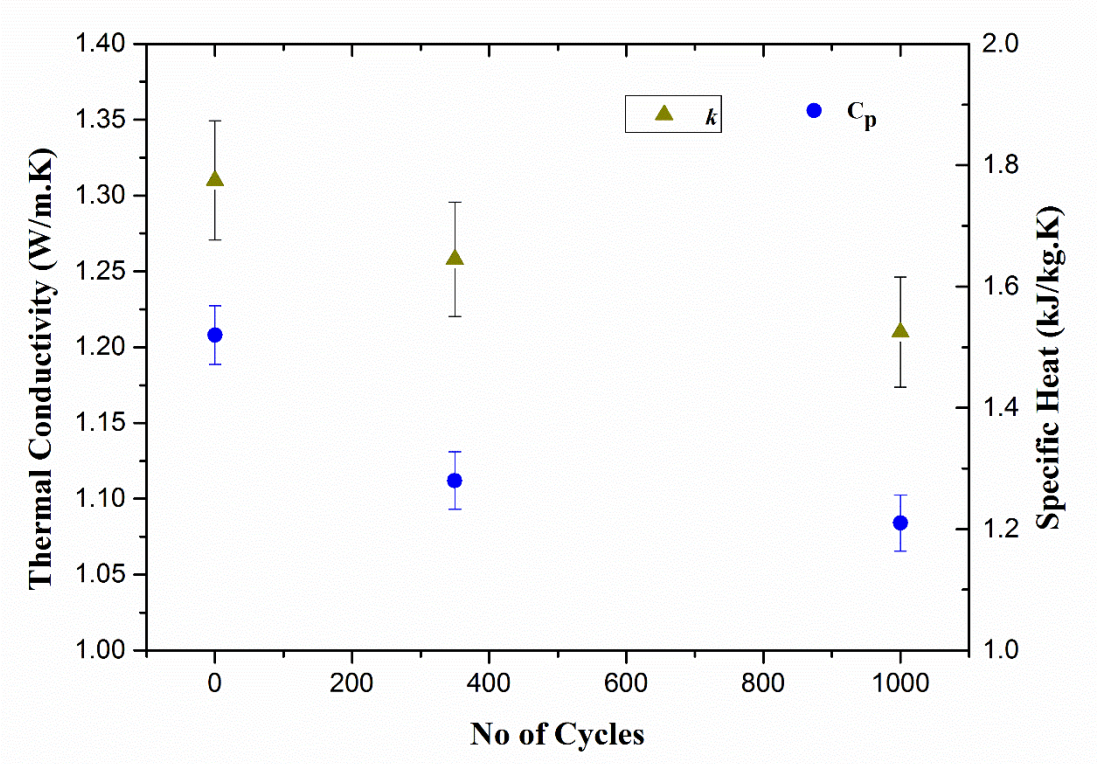

Fig. 3d. Thermal conductivity and specific heat of DM.

Fig. 3e shows the DSC data of DM before and after thermal cycles. Initially, the samples are in powder form. The powder is melted in the first run and reading are presented from the second run of the experiment. Test results showed two distant peaks related to melting and solidification of DM. Samples showed no secondary peaks However, this finding is different from that reported by Mojiri et al. [28] in which they reported two exothermic peaks during solidification. They hypothesised polymorphic phase change and non-uniform solidification in the tablet for this observation. However, the quality of samples used may also effect the testing results. The melting point was found to be at 168.38 °C with latent heat enthalpy of 281.9 kJ/kg. Similarly, during cooling cycle, the solidification temperature was found at 118.55 °C with latent heat release of 219.52 kJ/kg. The phase change properties arein good agreement with other published data. Laia et al. [33]. As expected, there is a decrease in latent change of enthalpies of the PCM after thermal cycling due to slight oxidation of the material. The latent heat of melting and solidification were found to be 209.34 kJ/kg and 165.23 kJ/kg, respectively, after 1000 thermal cycles which results in 26% and 25% reduction in latent heat value after thermal cycle.

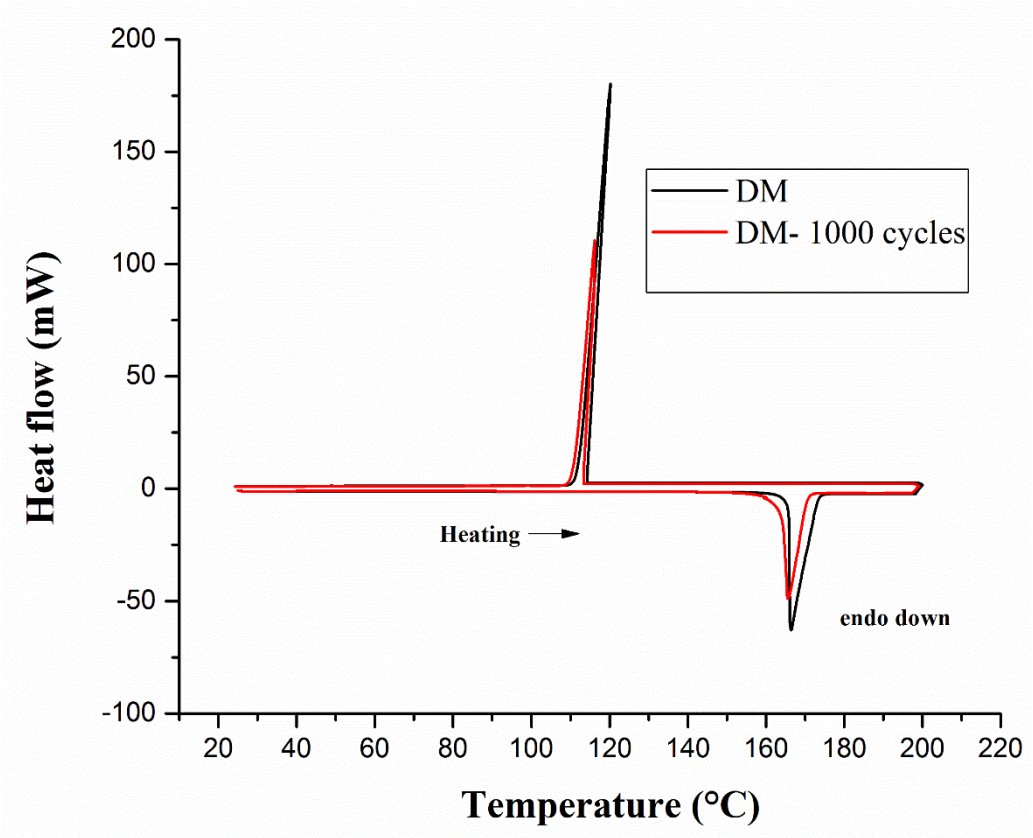

Fig. 3e. DSC data of DM

Table 2. The DSC results for DM for fresh and thermal cycled samples

Sample	Thermal cycles	Temperatures (°C)				Latent heat Capacity (kJ/kg)	
		Heating		Cooling			
		Onset(°C)	Peak(°C)	Onset(°C)	Peak(°C)	Melting	Solidification
DM	0	166.38	168.38	120.15	118.55	281.89	219.52
	1000	164.34	166.45	118.75	116.54	209.34	165.23

The FTIR spectra of DM are presented in Fig. 3f.FTIR analysis investigate the chemical stability of PCM after repeated thermal cycles. In the range of 3200 cm^{-1} and 3600 cm^{-1} a broad peak is observed which is attributed to the stretching frequency of O-H functional group (3280 cm^{-1} with 58.49 %). Peaks at 2942 cm^{-1} with 74.85 % transmittance can be attributed to the frequency of CH_3, $CH_2$and CH. The peaks showed that there is no discrepancy with studies conducted by Sole et al. [34]. After thermal cycles, similar peaks were observed but with change in transmittance. This may be due to the dehydration of sample after thermal cycling. From the spectra obtained, it is evident that DM is chemically stable after thermal cycles. Table. 3. Summarises the functional group of the DM with respective attribution.

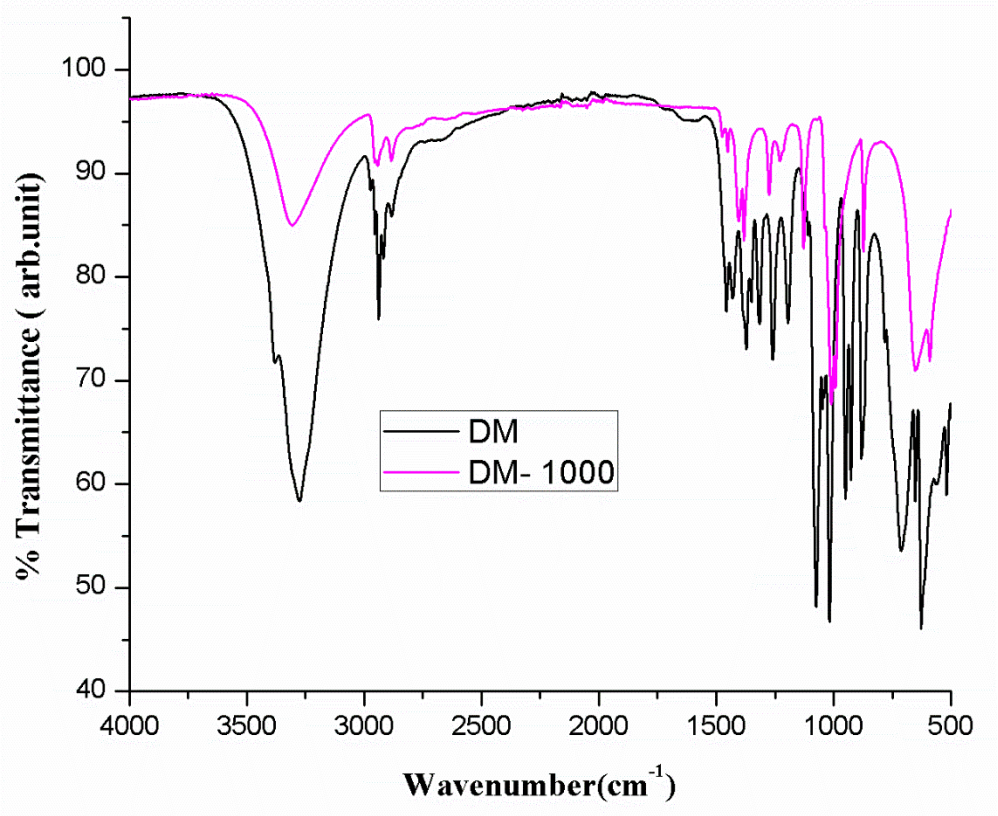

Fig. 3f. The FTIR results of DM.

Table 3. Functional group data of DM

Frequency (cm^{-1})	Functional Group
3000-3800	O-H (Stretch), H-bonded (strong, broad)
1500-3000	C-H (Stretching)
1300-1450	–CH, $–CH_2$ and CH_3 (Variable bending)

3.2 Macro-scale TES experimental analysis.

3.2.1 Repeatability Tests

Repeatability tests were conducted to investigate the consistency of the transient temperature readings of thermocouple. In this view, three independent charging experiments were conducted at 1.5 l/min - volume flow rate and constant inlet temperature of 200 °C. Temperature profiles of thermocouple placed at top right (R1), Left side (L1) and bottom (D1) of TES are plotted (Fig. 4a). It was observed that the readings obtained for different trial

experiments, show a similar trend. Hence, the reliability of test for further investigation can be assured.

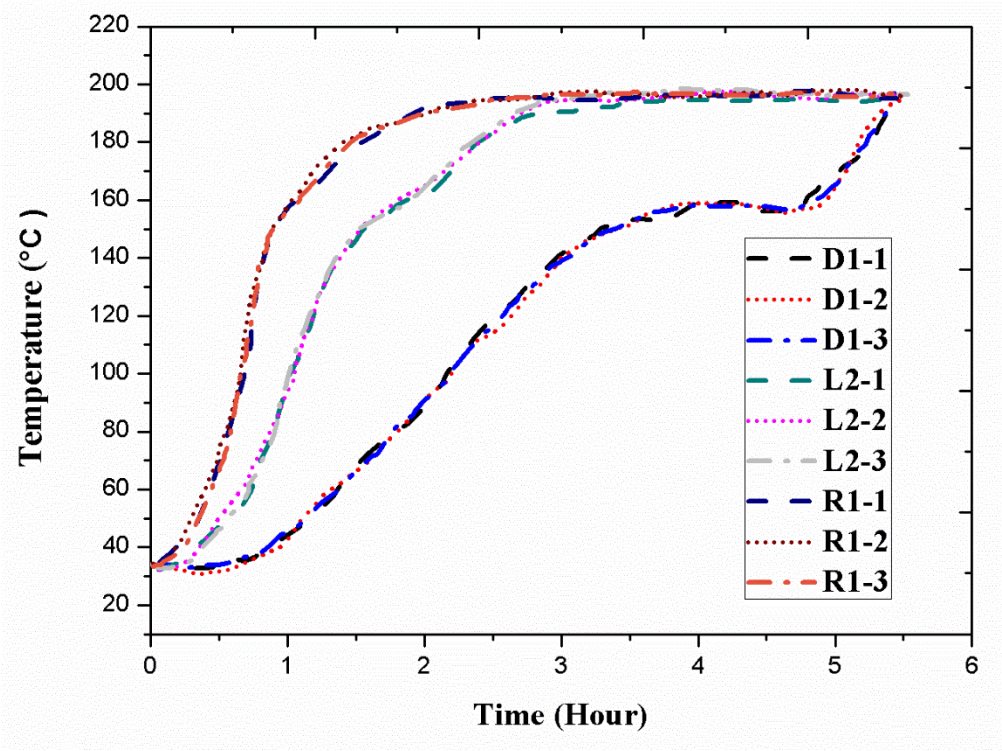

Fig. 4a. Repeatability tests – Temperature profiles of three different thermocouple readings

3.2.2 Inlet flow rate – Effect on charging and discharging time.

Tests at various flow rate of 0.5, 1.0, 1.5, 2 and3 l/min were conducted to investigate the effect of volume flow rate for charging and discharging process. Fig. 4 (c-d, e-f) shows the transient temperature profiles of temperature probes at two locations R1 and D1 for the charging and discharging cycle. It was observed from experimentation that R1 and D1 were the first and last thermocouple locations to melt during charging. All other temperature probes fall within the time limits of these two thermocouple probes. From Fig. 4(c-d), at an inlet temperature of 200 °C, it is seen that the initial rate of charging is very slow as compared to the latter stages. This is because the heat transfer is dominated by conduction during the start of the charging cycle. The low thermal conductivity of the PCM results in a lower heat transfer rate through the PCM. However, the heat transfer improves later due to the onset of natural convection in liquid PCM which in turn reduces the overall thermal resistance of the PCM. It is inferred from the results that with increase in flow rates, the time required for complete melting and solidification is decreased. By changing the flow rates

from 0.5 l/min, the phase transition time for charging was reduced by 14.1, 23.7, 24.3 and 24.6% for 1, 1.5, 2 and 3.0 l/min, respectively. Similarly, the discharging time was reduced by 26.5, 39.21, 39.28 and 39.33 %, respectively. It can be seen that the influence of varying inlet volume flow rate had more effect on discharging than during charging time. This is due to the major role played by natural convention of liquid PCM while the solidification majorly occurs due to conduction phenomenon. Furthermore, the change in time, when flow rate was changed from 0.5 to 1.5 l/min was drastic as compared to when the flow rate was increased to 2 and 3 l/min. This can be attributed to the HTF occupancy period in tubes, which reduces within creasing volume flow rates and hence, after certain volume flow rate units, the HTF tube surface remains at almost isothermal condition. Hence further increase in the volume flow rates has negligible effect on phase transition time for both charging and discharging. Hence for all further analysis in our analysis, we have taken a constant inlet volume flow rate of 1.5 l/min for both charging and discharging processes.

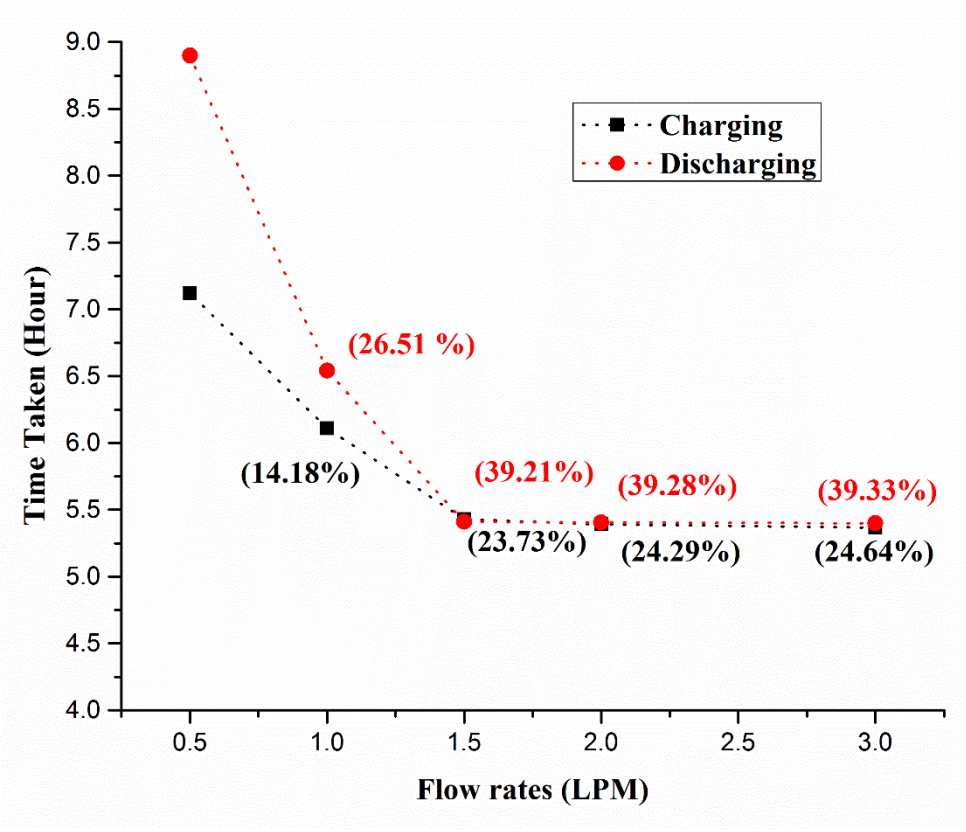

Fig. 4b. Time taken for complete charging and discharging of PCM vs. the volume flow rates of HTF.

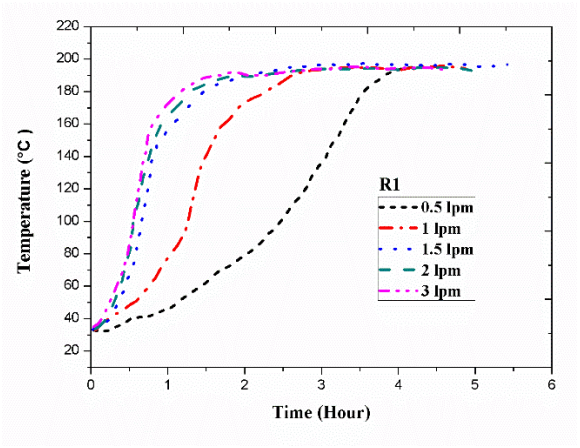

(4. c)

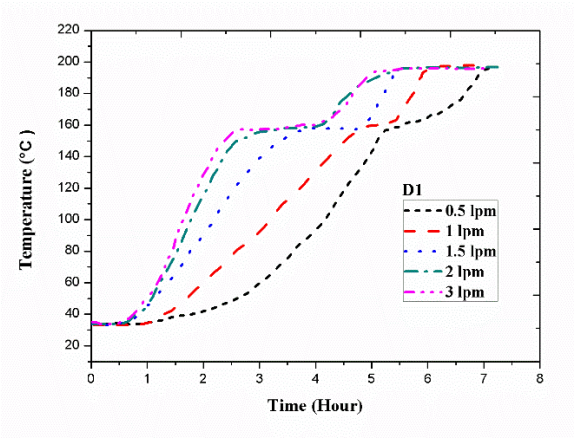

(4. d)

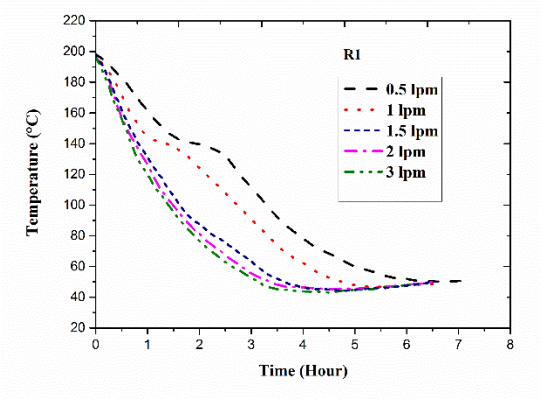

(4.e)

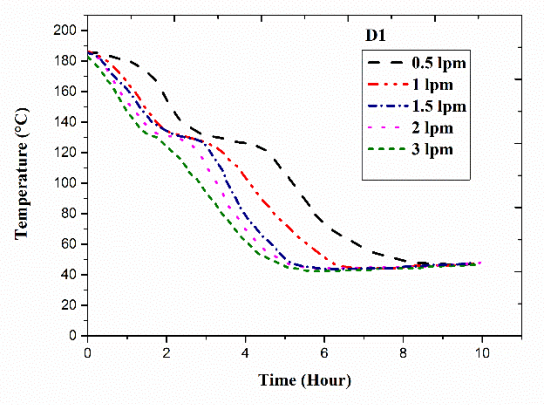

(4.f)

Fig. 4 (c-d). Temperature profiles at probe location R1 and D1 for different flow rates.

3.2.3. Effect of inlet temperature on charging and discharging time of TES

In practical conditions, the inlet temperature to TES may vary depending on fluctuating weather conditions. To study this effect, experiments were conducted at different inlet temperatures of 200 °C and 220 °C for charging cycle and 30 °C and 20 °C for discharging cycle at a constant volume flow rate of HTF at 1.5 l/min. Fig. 4g shows the photographic view of phase transition performance of PCM. The temperature profiles of PCM acquired from thermocouples installed at various locations are illustrated at Fig. 4(h-k). It is clear from the investigation that the HTF inlet temperature plays a significant role in charging and discharging process of the PCM. Higher the inlet temperature, greater is the temperature gradient of the PCM and the HTF. With more temperature gradient, higher heat transfer rate can be obtained which further leads to faster phase change from solid to liquid phase. Faster phase change is due to increase of liquid PCM which initiates quick natural convection in the

TES, thus leading to decrease in complete charging time. Fig. 4g shows the pictorial representation of charging and discharging of TES without insulation. During the charging process, the PCM first melts around the HTF tube and due to natural convection of liquid PCM, the top region of the TES melts first. From the pictures it is clear that the last region to melt is the bottom most part of the TES. During solidification, conduction heat transfer takes a major role and the PCM starts solidification on the HTF tube. The PCM is seen solidifying on the outer surface of the shell due to temperature gradient between the glass shell and atmospheric air. From Fig. 4h is it seen that the transition rate of PCM is greater for 220 °C when compared to 200 °C. When the inlet temperature was increased to 220 °C, the total melting reduced to 1.83 hrs. which amounts to a decrease in melting time by 23.7%. From the figure, it is clearly seen that the bottom part of TES melts last (D1). The total time taken for PCM at bottom position(D1) to melt is 5.43 hrs. With increase of inlet temperature to 220 °C, the melting time reduced to 3.89 hrs. which is a 28.3 % reduction in time. For central and bottom positions, the time taken for melting varied from 4.5 hrs. to 3.2 hrs. for 200 °C inlet temperature. Also, it can be inferred from the profiles that the central part is also affected due to the natural convention of PCM liquid molecules due to buoyancy effect. Thus, higher the inlet temperature, higher the phase transition rate of the PCM in all positions of the TES.

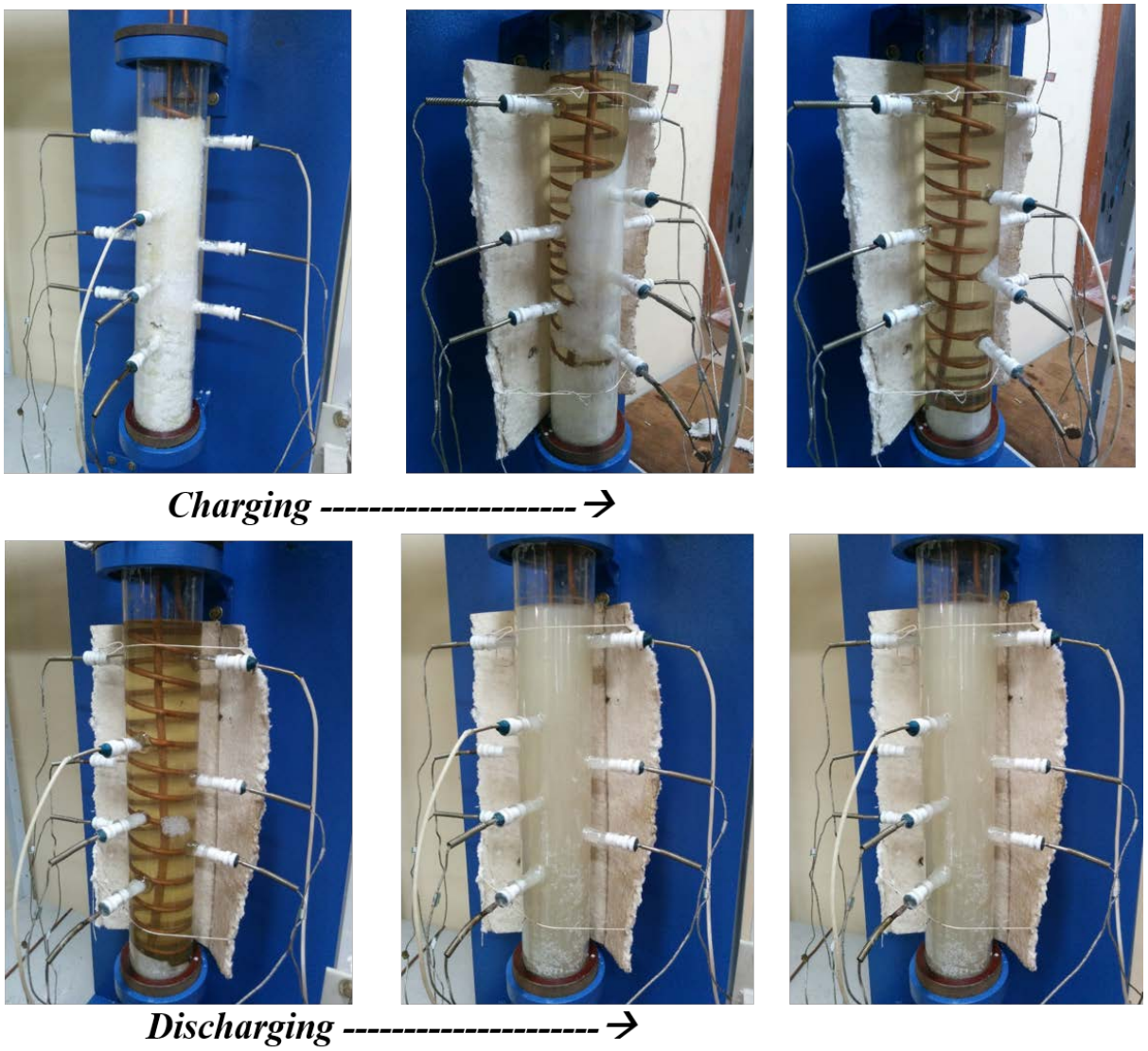

Fig. 4g Pictorial view melting and solidification behaviour of PCM during experimentation.

As seen during charging, the inlet HTF temperature also played a significant role during the discharging cycle. The transient temperature profiles of DM are as shown in Fig. 4(j-k). The sensible energy played a vital role due to domination of conduction heat transfer. For complete solidification of PCM at 30 °C, the time taken was 5.4 hrs. The total solidification time decreased to 4.79 hrs, which amounts to a 11.2 % enhancement when inlet temperature changed from 30 °C to 20 °C. The discharging rate of both the sensible heat and latent heat portion of PCM were at a higher rate when the inlet temperature was changed.

Furthermore, it is seen that the onset of solidification of DM starts at temperature range of 148-142 °C which suggests that on macro scale, DM solidifies at a lower subcooling temperature which is advantageous for its application as PCM in TES systems. Moreover, it

is also seen that the temperature range between all thermocouples is narrow during discharging. This is due to fact that during discharging, conduction plays a major role in heat transfer between the HTF and PCM.

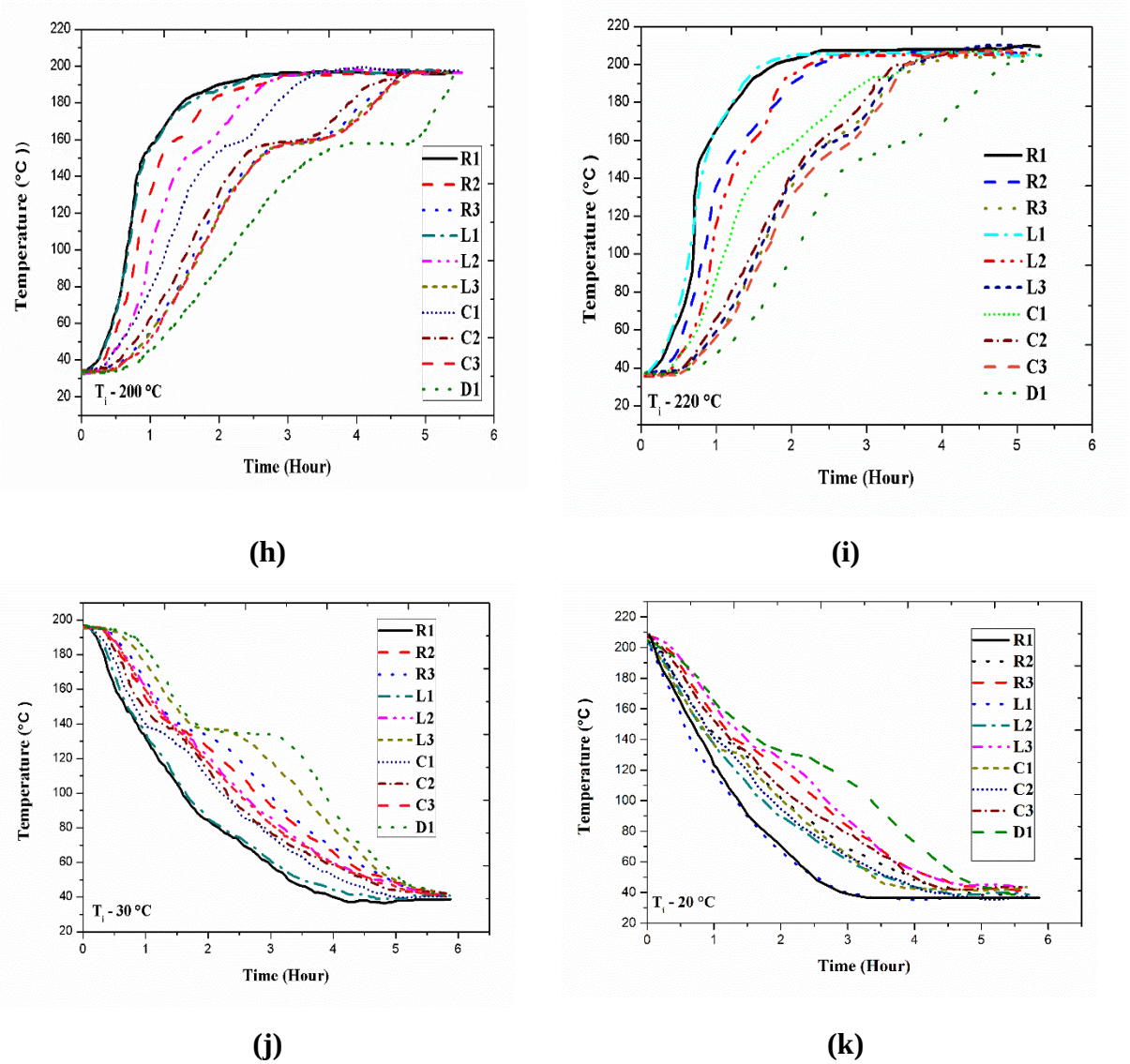

Fig. 4(h-k). Temperature variation of PCM at various operating conditions.

3.2.4. Effect of Ga laden in DM to form PCM composites

As discussed, the thermal response of the TES could be increased by addition of high thermal conductivity material in the PCM. For conducting experiments, gallium with 0.5 wt.% is added into DM and tested in the designed prototype. In our previous study [34], we had characterised the thermophysical properties of DM-Ga with 0.1wt.% and 0.5wt.% Ga composites. Results showed that the increase in thermal conductivity value of 0.1 wt.% Ga

was negligible as compared to DM-0.5 wt.% Ga composite. The value of 1.67 W/m·K was obtained for thermal conductivity for 0.5 wt.% Ga with 27.8 wt.% enhancement as compared to pristine DM. In this section we investigate the effect of Ga in DM on the charging and discharging performance of the prototype TES system. ·

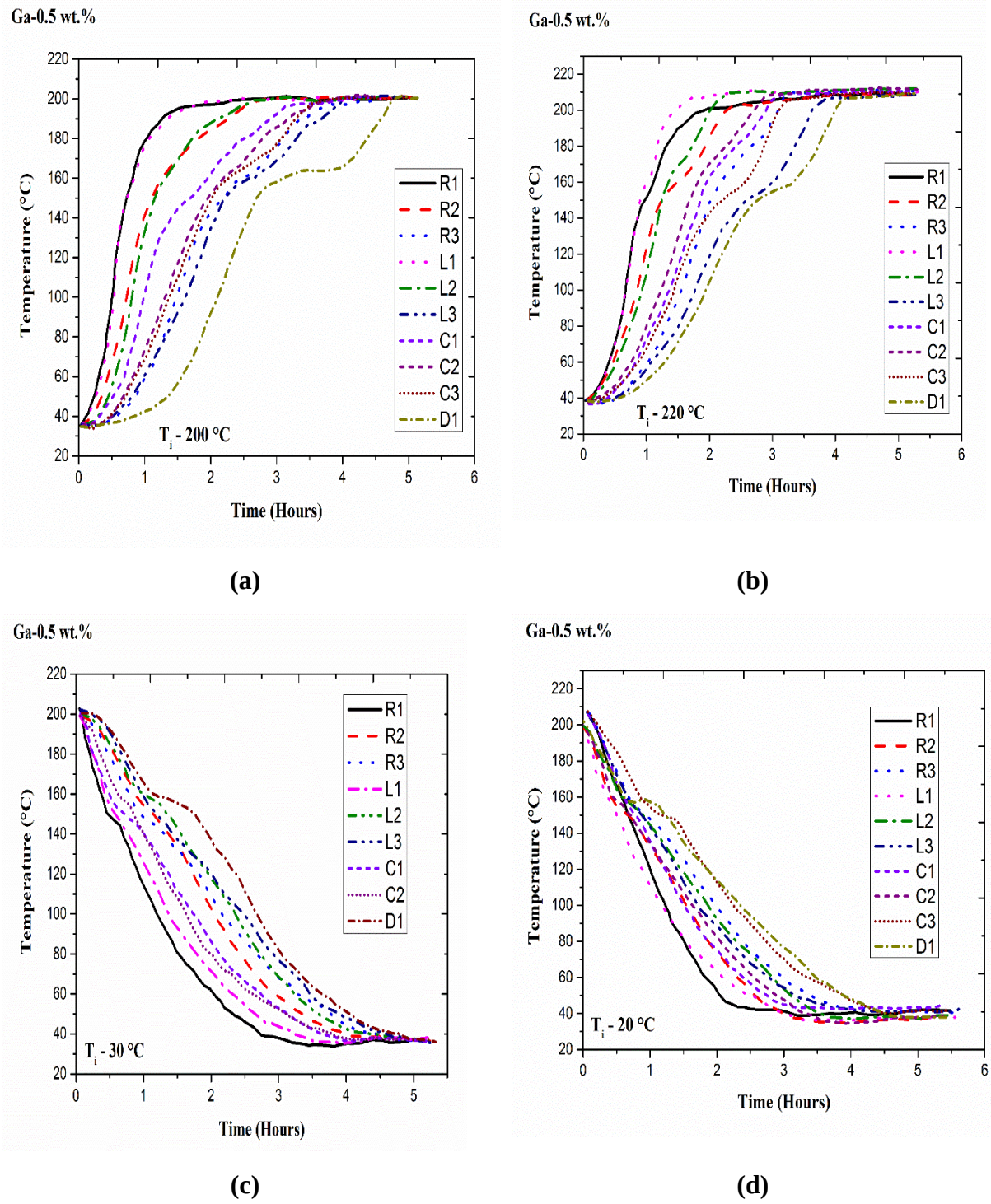

Fig. 5. Temperature variation of PCM in TES with DM-0.5 wt.% Ga composite

Fig.5 shows the transient temperature profiles of DM-Ga composite at respective zone in the TES for different operating temperatures. Comparing the profiles obtained with that of Fig. 4, it is clear that DM-Ga composite increased the heat transfer rate in the PCM. Both, during charging and discharging cycle, the profiles are narrower when compared to that of DM case. This is due to presence of Ga particles in the PCM sample space and grain boundaries of the PCM. For inlet temperature of 200 °C, the total time for R1 (top zone) and D1 (bottom zone) to reach melting is 1.56 hrs. and 4.89 hrs respectively. Similar for 220 °C, the time taken for corresponding zone was 1.48 and 3.51 hrs, which is 9.9% and 9.8% lesser as compared to time taken for DM. During discharging cycle, the total time taken for complete solidification was 4.81 hrs and 4.25 hrs. when the inlet temperature was maintained at 30 °C and 20°C respectively. As compared to pure DM case, for the corresponding inlet temperature, there was a reduction by 10.9% and 11.3% for complete solidification.

3.2.5. Effect of metal inserts with Ga in TES.

Response of the TES with DM-Ga composite was explored in the previous section. But the drawback with these techniques include a) Increase in weight of the heat exchanger with decreased economic benefits b) Reduction in latent heat capacity of PCM due to the addition of particles c) Challenges in disposal of composite PCM after its usage. Hence, in this paper, we investigate a new novel concept of using hollow metal inserts with gallium, inserted and assembled in TES. Four metal inserts are assembled in between the helical coil and the shell of the heat exchanger. Our research is limited to only four inserts due to increased interference of inserts with the thermocouples used to trace the transient temperature of PCM. About 100 ml of Ga is added to each metal insert. Gallium is chosen because of its very high thermal conductivity as well as low specific heat. Lower specific heat enables it to transfer heat from the surrounding at a faster rate. For assembling the metal inserts, the entire TES is charged to 200 °C so that the PCM is in liquid state. Then the 4 metal inserts are inserted from the top of the covering plate which has special slots with predefined pitch. The inserts are held in the top after assembly by ferrule nuts. The same operating parameters used in the previous section are used again for investigation. Fig.6 shows the transient temperature profile of PCM at respective zones in the TES. It is very clear from the profiles that due to the low specific heat capacity of metal inserts with Ga, the linear temperature rise is greater as compared to TES with plain metal inserts. This is influenced not only by conductive heat transfer through the copper metal inserts but also convective heat transfer by gallium inside the metal inserts. Hence in this design, during charging ,the heat transfer from HTF to PCM

is not only through PCM but also through copper metal inserts and liquid Ga. It is clear from Fig.6, as compared to TES without metal inserts, the temperature increases ata faster rate when metal inserts are used. The time required at the top zone (R1) for melting is 1.8 hrs. as compared to 2.4 hrs., for an inlet temperature of 200 °C. As seen in the previous section, the bottom zone of the TES is the last region to melt and the total time taken for melting is 4.11 hrs. This amounts to a 24.3% reduction in total time for completing charging as compared to TES without metal inserts. Fig.6b shows the temperature profile of PCM when the inlet temperature is maintained at 220 °C. As discussed in the previous section, all the zones showed increased heat transfer rates .The top zone(R1) melted first within 1.8 hrs. while bottom zone(D1) took 3.08 hrs. .As compared to TES without metal inserts and with 220 °C inlet temperature of HTF, there was a 20.78% reduction in charging time of the complete TES. Fig. 6c shows the transient temperature profile of PCM during the discharging cycle with an inlet temperature of 30 °C.

From the profiles, it is seen that the sensible heat rapidly discharges due to an enhanced temperature gradient. Presence of metal inserts further enhances the solidification process due to formation of nucleation sites around the external surfaces of the metal inserts and high heat transfer by the liquid Ga. It is important to note that although the PCM has solidified, the Ga is still in the liquid phase while help in heat transfer by the natural convection of Ga molecules inside the tube, thus maintaining a low temperature difference between HTF and PCM and thereby increasing the effectiveness of the TES. With metal inserts, the total time taken for discharging is 4.42 hrs. and 3.69 hrs for 30 °C and 20 °C inlet temperature, respectively. As compared to TES without inserts, for the same inlet temperature, the decrease in discharging time is calculated to be18.1% and 22.9%. This decrease in discharging time will enhance the power output of the TES and with added advantageous for application in solar thermal energy storage system.

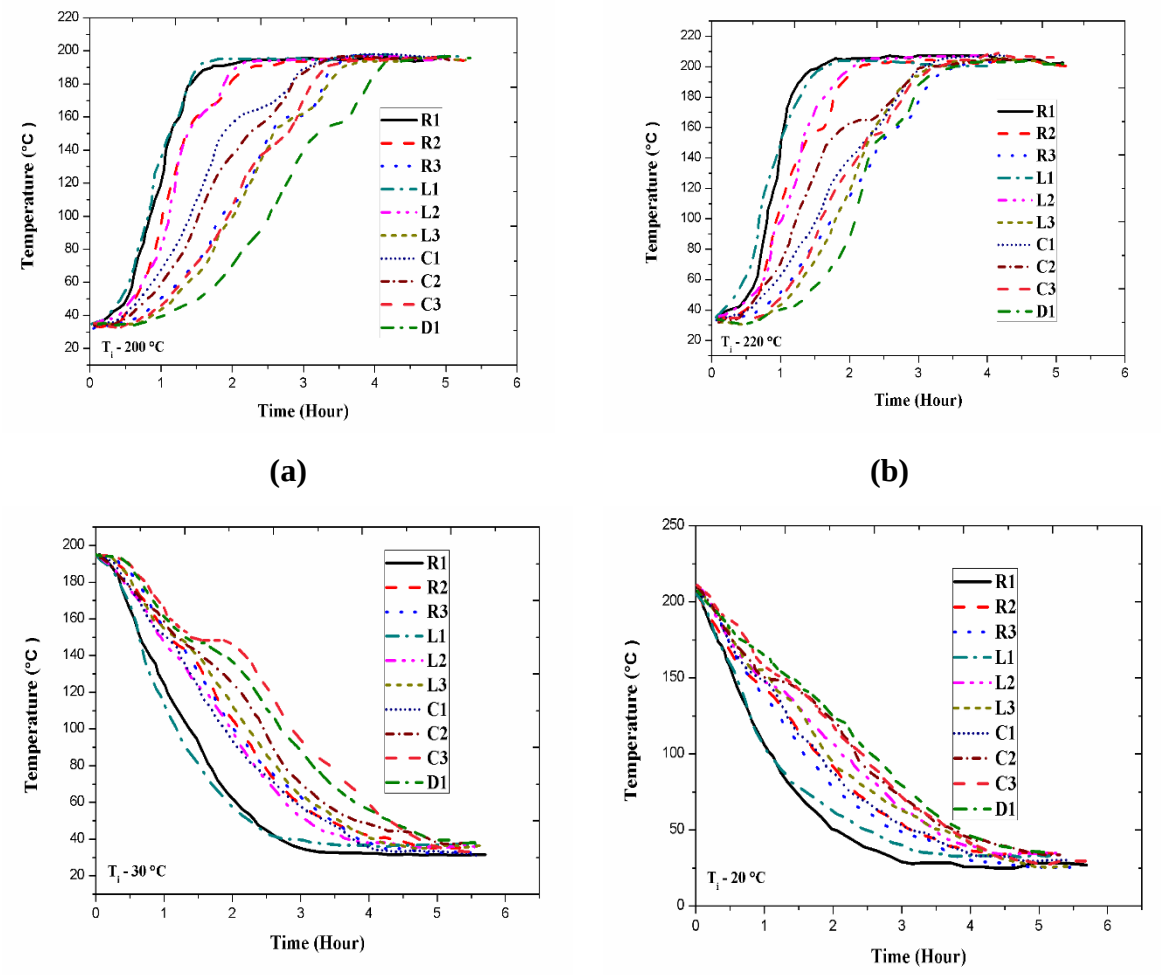

Fig. 6. Temperature variation of PCM in TES with metal inserts containing liquid metal gallium at various operating conditions.

3.2.6. Cumulative Energy and Mean Power

To investigate the thermal performance of DM in TES, with and without metal inserts with Gallium, the cumulative energy stored/ retrieved and mean power are calculated. The mass of the PCM and the volume flow rate of the HTF is constant for all cases investigated. Moreover, it is seen that for different operating conditions, the cumulative energy and mean

power are highly influenced by the time duration for charging and discharging. In the previous Section 3.2.4, it was clearly seen that addition of metal inserts have impacted the time for complete charging and discharging.

Moreover,after the addition of the metal inserts with Ga, the temperature gradient was reduced drastically due to the role played by liquid metal in transferring heat uniformly in sample space. As a result, a higher average mean power is generated with the presence of metal inserts with Ga. It was observed that during the charging process, for 200 °C inlet temperature, the mean power was0.4885 kW which further enhances to 0.694 kW when the inlet temperature was increased to 220 °C. During discharging cycles, the power released was0.433 kW for 30 °C inlet temperature and 0.4915 W for inlet temperature of 20 °C.

For case of DM-Ga with 0.5 wt.% composite, the mean power was found to be 0.53 and 0.75 kW for 200 °C and 220 °C during charging process. During discharging cycle, for 30 °C and 20 °C inlet temperature, the mean power was found to 0.45 kW and 0.54 kW. TES with metal inserts with Ga showed enhanced mean power performance as compared to TES without metal inserts. For 200 °C inlet temperature, 0.6481 kW of mean power was calculated. This amount to an increase of32.6 % as compared to without metal inserts. When the inlet temperature was increased to 220 °C, the mean power was found to 0.8788 kW. Similarly during discharging cycle, for 30 °C inlet temperature, 0.531 kW of power was discharged and 0.6404 kW was discharged for inlet temperature of 20 °C. The mean power is tabulated and summarised in Table 4.

Table 4. Mean Power of TES with and without Metal Inserts.

	Mean Power (kW)		
Inlet Temp.	***Without Inserts***	***DM-Ga composite***	***With Ga. Inserts***
200 ℃	0.4885	0.537(9.9%)	0.6481 (32.6 %)
220 ℃	0.6949	0.751(8.18%)	0.8788 (26.47 %)
30 ℃	0.4336	0.45(5.2%)	0.5310 (22.46 %)
20 ℃	0.4915	0.542(10.3%)	0.6404 (30.2 %)

3.2.6 Efficiency

The theoretical efficiency and total efficiency were calculated to investigate the heat transfer performance of the TES with and without metal inserts with gallium. Neglecting the subcooling effect of DM, the total theoretical energy storage capacity of PCM is 13.29 MJ. Table 5-6 presents detailed quantitative data regarding the experiments conducted. From the Table 5. it can be seen that with an increase in inlet HTF, the theoretical efficiency increases. Maximum efficiency was calculated to 73.42 % and 64.07 % for charging and discharging of TES with Ga in metal inserts with 220 °C and 20 °C as the inlet HTF temperatures, respectively. These values are obtained as per equation 5 described in the Section 2.5. These represent the energy stored/discharged at respective operating conditions as compared to the maximum amount of energy storage/discharge possible. Table 6. shows the total efficiency of the TES. From the table, it can be seen that for 220 °C inlet temperature of charging and 20 °C discharging temperature, the efficiency is 87.26%. While the highest efficiency is for TES with Ga with 200 °C (charging) and 20 °C (discharging) with 88.79 %. This shows that decreasing the inlet HTF during discharging temperature has a larger effect on the total efficiency than increasing the HTF temperature during charging. However, based on the power demand and temperature of HTF output required, the TES should be optimally designed.

Table 5. The effect of inlet HTF temperatures on the theoretical efficiency.

		DM		**DM-Ga composite**		**Metal Inserts with Ga**	
Theoretical Efficiency	**Charging**	**200 °C**	**220 °C**	**200 °C**	**220 °C**	**200 °C**	**220 °C**
	%	*71.8*	*73.2*	*71.1*	*71.4*	*72.1*	*73.4*
	Discharging	**30 °C**	**20 °C**	**30 °C**	**20 °C**	**30 °C**	**20 °C**
	%	*63.4*	*63.8*	*59.4*	*62.4*	*63.6*	*64.0*

Table 6. The effect of inlet HTF temperatures on the total efficiency.

		Total Efficiency (%)	
	T_{in} (Charging)	**T_{in} -30 °C**	**T_{in} -20 °C**
DM	**200 °C**	*88.27*	*88.85*
	220 °C	*86.55*	*87.11*

DM+ Ga composites	**200 °C**	*83.5*	*87.7*
	220 °C	*83.1*	*87.3*
Metal Inserts with Ga	**200 °C**	*88.27*	*88.79*
	220 °C	*86.75*	*87.26*

4. Conclusion

In this paper, the thermal performances of novel TES unit with metal inserts were experimentally investigated at various operating conditions using D-Mannitol as phase change material. Liquid metal gallium in metal inserts were assembled in the TES to check its effect on the thermal performance of TES. Based on experimental results, the following conclusions were derived.

- D-Mannitol showed a latent heat capacity of 285 kJ/kg and has a melting temperature range of 165-168 °C. After 1000 thermal cycles, the latent heat capacity decreased to 167 kJ/kg.
- DM showed physical and thermal stability after thermal cycles. FTIR data showed its chemical stability. Mass loss were negligible and were below 3% in the working temperature range.
- Due to vertical orientation of the TES, major role in melting process was played by natural convection. This can be attributed to up surge of high temperature PCM liquid molecules due to density differences. This allows the heat transfer to be dominated by convection. Convection had played no role during the discharging process. The dominant mode was conduction heat transfer. Heat transfer was rapid at the top zone of the TES and relatively weak at the bottom zone.
- Novel design configuration which includes the assembly of metal inserts with liquid metal gallium enhanced the overall heat transfer of TES. Results showed that the novel design ensured an enhanced energy storing capacity with higher process completion rates. 9.75 MJ of energy was stored in 3.08 hours when the TES was charged at an inlet temperature of 220 °C.
- In TES, D-Mannitol began solidify at the temperature range of 150-140 °C, which suggests that in major scale TES setup, the crystallization starts at higher temperature

range, thereby reducing the subcooling temperature and is suitable for usage as PCM in TES application.

- A maximum mean power of 0.878 kW was seen for TES with metal inserts atinlet temperature of 220 °C.

With further efforts to negate subcooling temperatures and with the elimination of degradation of latent heat enthalpies under thermal cycling, DM can be considered suitable for latent heat PCM for TES applications. Moreover, the proposed novel TES design with metal inserts with liquid metal Gallium can be universally used to test any PCM with anytemperature range of applications. Furthermore, the gallium used can be processed and reused for other applications. Likewise, the novel TES is very easy to assemble and disassemble. Depending on the energy demands and mean power, the TES may be assembled in parallel and used in a variety of commercial applications like solar thermal and industrial waste heat recovery units.

Acknowledgment

This work is sponsored by DST-SERI, Government of India, Ref. No:DST/TM/SERI/DSS/275(G); dated September 9, 2015. In addition, the authors would like to acknowledge the funding acquired from UKIERI-DST (IND/CONT/GA/18-19/16), which made this research possible.

Declarations of interest

None

Reference

[1] K. Pielichowska, K. Pielichowski, Phase change materials for thermal energy storage, Prog. Mater. Sci. 65 (2014) 67–123.

[2] C. Liu, Z. Rao, J. Zhao, Y. Huo, Y. Li, Review on nanoencapsulated phase change materials: Preparation, characterization and heat transfer enhancement, Nano Energy. 13 (2015) 814–826.

[3] J. Chen, J. Li, H. Wang, W. Huang, W. Sun, T. Xu, Preparation and effectiveness of composite phase change material for performance improvement of Open Graded Friction Course, Journal of Cleaner Production. 214 (2019) 259–269.

[4] L. Miro, J. Gasia, L.F. Cabeza, Thermal energy storage (TES) for industrial waste heat (IWH) recovery : A review, 179 (2016) 284–301.

[5] Z. Zhou, J. Liu, C. Wang, X. Huang, F. Gao, S. Zhang, B. Yu, Research on the Application of Phase- change Heat Storage in Centralized Solar, Journal of Cleaner Production. (2018).

[6] Y. Zheng, W. Zhao, J.C. Sabol, K. Tuzla, S. Neti, A. Oztekin, J.C. Chen, Encapsulated phase change materials for energy storage - Characterization by calorimetry, Sol. Energy. 87 (2013) 117–126.

[7] M. Dadollahi, M. Mehrpooya, Modeling and investigation of high temperature phase change materials (PCM) in different storage tank configurations, Journal of Cleaner Production. 161 (2017) 831–839.

[8] Jesumathy SP, Udayakumar M, Suresh S, Jegadheeswaran S. An experimental study on heat transfer characteristics of paraffin wax in horizontal double pipe heat latent heat storage unit. Journal of the Taiwan Institute of Chemical Engineers. 2014 Jul 1;45(4):1298-306.

[9] Z. Jiang, T. Ouyang, Y. Yang, L. Chen, X. Fan, Y. Chen, W. Li, Y. Fei, Thermal conductivity enhancement of phase change materials with form-stable carbon bonded carbon fiber network, Mater. Des. 143 (2018) 177–184.

[10] D.D.W. Rufuss, L. Suganthi, S. Iniyan, P.A. Davies, Effects of nanoparticle-enhanced phase change material (NPCM) on solar still productivity, Journal of Cleaner Production. (2018).

[11] J. Gasia, L. Miro, L.F. Cabeza, Materials and system requirements of high temperature thermal energy storage systems : A review . Part 2 : Thermal conductivity enhancement techniques, Renew. Sustain. Energy Rev. 60 (2016) 1584–1601.

[12] Venkitaraj KP, Suresh S, Praveen B. Energy storage performance of pentaerythritol blended with indium in exhaust heat recovery application. Thermochimica Acta. 2019 Oct 1;680:178343.

[13] A. Jamekhorshid, S.M. Sadrameli, M. Farid, A review of microencapsulation methods of phase change materials (PCMs) as a thermal energy storage (TES) medium, Renew. Sustain. Energy Rev. 31 (2014) 531–542.

[14] Praveen B, Suresh S. Thermal performance of micro-encapsulated PCM with LMA thermal percolation in TES based heat sink application. Energy conversion and management. 2019 Apr 1;185:75-86.

[15] A. Sari, A. Karaipekli, Thermal conductivity and latent heat thermal energy storage characteristics of paraffin/expanded graphite composite as phase change material, Appl. Therm. Eng. 27 (2007) 1271–1277.

[16] A.A. Ranjbar, S. Kashani, S.F. Hosseinizadeh, M. Ghanbarpour, Numerical heat transfer studies of a latent heat storage system containing nano-enhanced Phase Change Material, Therm. Sci. 15 (2011) 169–181.

[17] S.F. Hosseinizadeh, A.A.R. Darzi, F.L. Tan, Numerical investigations of unconstrained melting of nano-enhanced phase change material (NEPCM) inside a spherical container, Int. J. Therm. Sci. 51 (2012) 77–83.

[18] A.A.R. Darzi, M. Farhadi, K. Sedighi, Numerical study of melting inside concentric and eccentric horizontal annulus, Appl. Math. Model. 36 (2012) 4080–4086.

[19] K.A.R. Ismail, C.L.F. Alves, M.S. Modesto, Numerical and experimental study on the solidification of PCM around a vertical axially finned isothermal cylinder, Appl. Therm. Eng. 21 (2001) 53–77.

[20] M.J. Hosseini, M. Rahimi, R. Bahrampoury, Experimental and computational evolution of a shell and tube heat exchanger as a PCM thermal storage system, Int. Commun. Heat Mass Transf. 50 (2014) 128–136.

[21] N.R. Vyshak, G. Jilani, Numerical analysis of latent heat thermal energy storage system, Energy Convers. Manag. 48 (2007) 2161–2168.

[22] H.A. Adine, H. El Qarnia, Numerical analysis of the thermal behaviour of a shell-and-tube heat storage unit using phase change materials, Appl. Math. Model. 33 (2009) 2132–2144.

[23] G. Peiró, J. Gasia, L. Miró, L.F. Cabeza, Experimental evaluation at pilot plant scale of multiple PCMs (cascaded) vs. single PCM configuration for thermal energy storage, Renew. Energy. 83 (2015) 729–736.

[24] M. Rahimi, A.A. Ranjbar, D.D. Ganji, K. Sedighi, M.J. Hosseini, R. Bahrampoury, Analysis of geometrical and operational parameters of PCM in a fin and tube heat exchanger, Int. Commun. Heat Mass Transf. 53 (2014) 109–115.

[25] M. Esapour, M.J. Hosseini, A.A. Ranjbar, R. Bahrampoury, Numerical study on geometrical specifications and operational parameters of multi-tube heat storage systems, Appl. Therm. Eng. 109 (2016) 351–363.

[26] Z. Khan, Z.A. Khan, Experimental investigations of charging/melting cycles of paraffin in a novel shell and tube with longitudinal fins based heat storage design solution for domestic and industrial applications, Appl. Energy. 206 (2017) 1158–1168.

[27] Z. Khan, Z.A. Khan, An experimental investigation of discharge/solidification cycle of paraffin in novel shell and tube with longitudinal fins based latent heat storage system, Energy Convers. Manag. 154 (2017) 157–167. [25] A. Mojiri, N. Grbac, B. Bourke, G. Rosengarten, D-mannitol for medium temperature thermal energy storage, Sol. Energy Mater. Sol. Cells. 176 (2018) 150–156.

[28] H. Niyas, S. Prasad, P. Muthukumar, Performance investigation of a lab–scale latent heat storage prototype – Numerical results, Energy Convers. Manag. 135 (2017) 188–199.

[29] Y. Grosu, A. Faik, I. Ortega-Fernández, B. D'Aguanno, Natural Magnetite for thermal energy storage: Excellent thermophysical properties, reversible latent heat transition and controlled thermal conductivity, Sol. Energy Mater. Sol. Cells. 161 (2017) 170–176.

[30] M. Karthik, A. Faik, P. Blanco-Rodríguez, J. Rodríguez-Aseguinolaza, B. D'Aguanno, Preparation of erythritol-graphite foam phase change composite with enhanced thermal conductivity for thermal energy storage applications, Carbon N. Y. 94 (2015) 266–276.

[31] E.P. del Barrio, A. Godin, M. Duquesne, J. Daranlot, J. Jolly, W. Alshaer, T. Kouadio, A. Sommier, Characterization of different sugar alcohols as phase change materials for thermal energy storage applications, Sol. Energy Mater. Sol. Cells. 159 (2017) 560–569.

[32] L. Miro, C. Barreneche, G. Ferrer, A. Solé, I. Martorell, L.F. Cabeza, Health hazard, cycling and thermal stability as key parameters when selecting a suitable phase change material (PCM), Thermochim. Acta. 627–629 (2016) 39–47.

[33] A. Sole, H. Neumann, S. Niedermaier, I. Martorell, P. Schossig, L.F. Cabeza, Stability of sugar alcohols as PCM for thermal energy storage, Sol. Energy Mater. Sol. Cells. 126 (2014) 125–134.

[34] Salyan S, Suresh S. Liquid metal gallium laden organic phase change material for energy storage: an experimental study. International Journal of Hydrogen Energy. 2018 Jan 25;43(4):2469-83.